

“ P- AND S-WAVE ATTENUATION IN THE KOPILI REGION OF NORTHEASTERN INDIA ”

Nilutpal Bora¹ and Rajib Biswas^{*,1}

⁽¹⁾ Geophysical Lab, Department of Physics, Tezpur University, Tezpur, Assam, India

Article history

Received September 6, 2018; accepted February 5, 2019.

Subject classification:

Attenuation; Seismic wave; Propagation; Quality factor; Heterogeneity.

ABSTRACT

We comprehensively analyze attenuation factor in Kopili region and its neighboring area. Corresponding to influence of frequency on attenuation, Q_p and Q_s are estimated from direct P and S waves. The results establish higher values of Q for S waves ($Q_s=(101\pm4)f(1.4\pm0.05)$) than for P waves ($Q_p=(45\pm3)f(1.3\pm0.07)$) in the 1.5-12 Hz frequency band. It is seen that our findings agree with other published results on tectonically active regions that is characterized by high degree of heterogeneity. Hence, it can be useful for further studies in ground motion prediction in Kopili region. The low value of quality factors corresponding to P and S waves refers to seismically active areas with complex heterogeneity. The estimated value of Q_s/Q_p and their subsequent association with frequency affirm the dominance of scattering as a major contribution to diminution of seismic amplitudes. This is further corroborated by local geological settings.

1. INTRODUCTION

Seismic waves are in general influenced by path effect, source effect and site effect. While propagating, there occurs diminution of amplitudes as well as energy of these seismic waves. This is referred to as seismic attenuation, designated by the term Q^{-1} . Seismic attenuation arises basically from two constituents, viz, body and coda waves. Between them, attenuation from body waves bears signature of the formation and material state of the interior part of the Earth [Sato, 1992].

Again, attenuation from body waves has got paramount importance in the prediction of ground motion parameters. The causes for attenuation can be various factors. Geometrical spreading and redistribution of seismic energy due to its passage through diverse medium need special mention [Tsujiura, 1966; Aki, 1969,1980; Aki and Chouet, 1975; Sato and Fehler,

1998; Mukhopadhyay et al., 2010].

The quality factor Q attempts to quantify the diminution of progressive seismic amplitudes from source to receiver site. Q also relates to the energy dissipation in accordance with Knopoff and Hudson [1964], Aki and Chouet [1975]. Sato and Fehler [1998] reported that seismic activity of a region can be classified with magnitude of Q where lower Q characterizes higher activity and lower activity is implied by greater magnitude of Q .

Q also bears direct correspondence with total harmonic wave energy. The harmonic wave energy is mathematically expressed as: $2\pi/Q=-\Delta E/E$ [Knopoff and Hudson, 1964], where E denotes total energy available in the harmonic wave and ΔE is the energy lost per cycle. Since P and S wave are manifested by varying seismic energies, body wave quality factors also exhibit different characteristics. Throughout the world, researchers have adopted diverse techniques to study quality factors [Aki,

1980; Sato and Matsumura, 1980; Hough and Anderson, 1988; Masuda, 1988; Takemura et al., 1991; Campillo and Plantet, 1991; Scherbaum and Sato, 1991; Yoshimoto et al., 1993; Yoshimoto et al., 1998].

To mitigate the seismic hazard of future calamitous earthquakes, a good understanding of attenuation and properties of the medium is required. To measure the attenuation, various methods have been devised from different portions of the seismograms [e.g., Aki, 1969; Hermann, 1980; Mitchell, 1995]. Wu [1985] suggested a technique from the dependence of total S-wave energy on hypocentral distance, for the assessment of the relative impact of scattering and intrinsic attenuation. Frankel and Wennerberg [1987] used the energy flux model of coda portion of the seismogram to obtain attenuation quality factor based on decay of coda amplitude. Hoshiba et al. [1991] developed a method based on Monte Carlo simulations of the temporal shape of the coda envelope. Aki [1980] introduced the coda normalization method, based on the idea that coda waves consist of scattered S-waves from random heterogeneities in the Earth. Sato and Matsumura [1980] adopted Aki's method to a set of deep borehole data. This method was extended by Yoshimoto et al., [1993] for simultaneous measurement of Q_p and Q_s .

In this paper, we compute frequency-dependent Q_p and Q_s in Kopili region, India. This part is one of the highly seismically active part in North-east India. To gain further insight into the seismic attenuation mechanism of this region, the extended coda-normalization method proposed by Yoshimoto et al., [1993] was used to determine Q_p and Q_s . This is the first application of the technique to this region. We also examine Q_s/Q_p ratio and its possible implications for its variation. The findings are also being matched with existing data of dissimilar regions of the sphere and inferred.

2. SEISMOTECTONICS OF KOPLI REGION

North east India has been established as one of the seismically active regions in the world with complex tectonic settings. As per reports [Kayal et al., 2006], seismic activity could be attributed to considerable deformation and reactivation of some faults during Quaternary period in Northeastern India. There were occurrences of two great earthquakes 1897 (MS 8.7) [Oldham, 1899] and 1950 (MS 8.6) [Poddar, 1950] and 16 large (MS=7.0) earthquakes within the last century. The

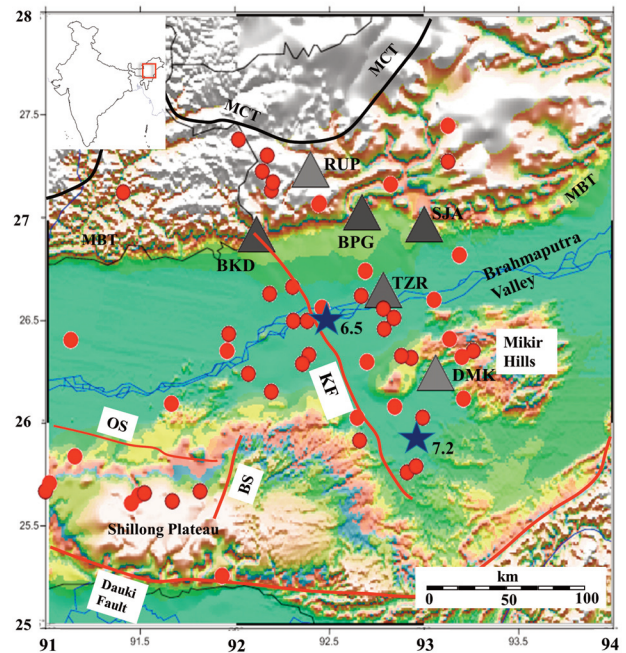


FIGURE 1. Map of Kopili Fault region [after Biswas et al., 2013a,b; Bora and Biswas, 2019]. The red circles symbolize the used events for this study, while triangles represents the temporarily deployed stations. The Great and major earthquakes occurred in and around this region was represented by the blue star symbol. (In inset the India map was shown).

region under study, Kopili Fault (KF) is encircled by diverse geological units. As for instance, the Himalayan frontal is situated to the north. Again, towards east, there exists highly folded Burmese arc. Besides, towards north, the main constituents comprise of thick sediments of Bengal. Among those earthquakes, KF had witnessed major event having magnitudes greater than seven [Biswas et al., 2018 a,b].

KF region is bounded by latitude 25.5° to 27° N and longitude 92° to 93° E. Additional evidence of seismic activity is borne by the earthquake of magnitude ~7.8 (MS), occurring at 60 km along KF on 10th of January 1869 [Kayal et al., 2010; Bora et al., 2017 a]. This wrecked a huge portion of areas between Silchar and Nagaon. On the same note, another event of 7.3 (MS) (27.5°N: 93.5°E) seemed to originate along KF on the year 1943. Recently, Kumar et al., [2016] reported that the entire region originated during the transition from Mesozoic to Tertiary period. Within this transition, rivers Kopili and Kalang had been channeling through this part, causing broad topographic depression (Figure 1). This KF possesses approximately width and length of 50 km and 300 km, respectively, covering Manipur, Arunachal Pradesh, Bhutan and Assam. According to

Kayal et al., [2006] and Kayal et al., [2010], KF is characterized by high seismic activity with events at a depth ~ 50 km. Bhattacharya et al., [2008] showed the depth of Kopili fault to range from 20 to 30 km. A high VP value at a depth of 40 km beneath Mikir Hills was also assessed by them. Meanwhile, Kundu and Gahalaut [2013] computed the active deformation of this fault as 2.9 ± 1.5 mm per year (Slip rate). As reported by Kayal et al., [2006 and 2010], this fault was a normal strike slip fault, having a dip towards the N-E side.

3. DATASET

In this study, we have utilized 300 digital seismograms generated by events with magnitude ranging from 1.9 to 3.9 in ML. We have selected 6 stations as shown in Figure 1. All these stations are maintained by various Government agencies and institutions [National Geophysical Research Institute, India Meteorological department and NEIST-Jorhat]. This network of six stations possessed GPS-synchronized Broadband Seismographs. The data was acquired at a sampling frequency

of 100Hz. The scattering of epicenters pertinent to this study is portrayed in Figure 1. Out of these 300 digital seismograms, only 192 seismograms have been chosen in order to study the attenuation mechanism in the study region within an epicentral distance up to 180 km and having a depth between 8.3 to 42 km. The Figure 2, represents an example of signal to noise ratios of different parts of the seismogram. We selected the events such that they must have a good signal to noise ratio. The selected events are randomly distributed, so that the radiation pattern can be least significant [Negi et al., 2014].

The onset of P and S wave are considered with the aim of deriving the wave spectra. Since we have selected events with small epicentral distances, the difference between S and P wave arrivals has been relatively trivial. This has led us to choose small sample lengths. The reason behind this step is to rule out P-wave contamination as much as possible. Prior to the selection of sampling length, we implemented baseline correction and eventually removal of trend line. A customized Matlab FFT code has been applied to compute the wave spectra by incorporating instrument correction.

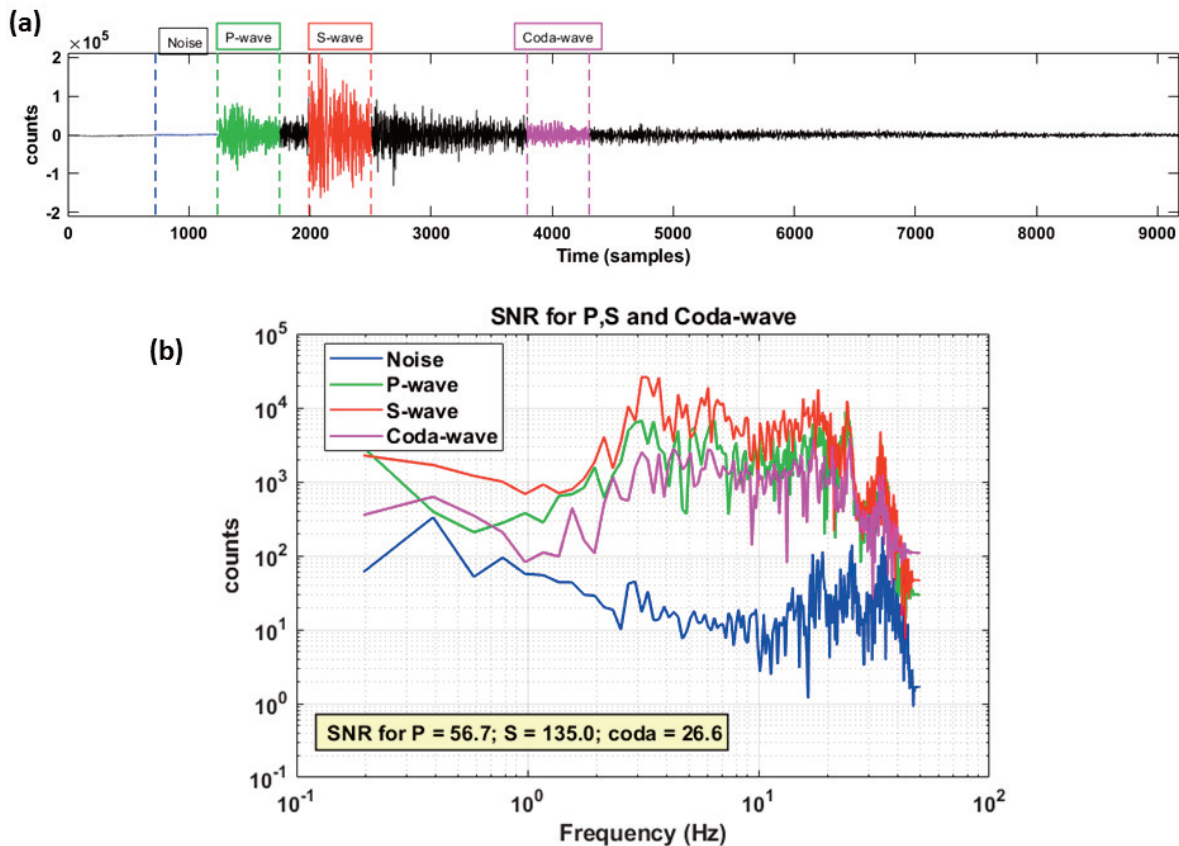


FIGURE 2. (a) The plot of typical seismogram. The colors represent the corresponding portions of the seismogram. (b) Signal to Noise ratios of corresponding portions for an recorded event at TZR station.

4. METHODOLOGY

In delineating attenuation characteristics, we implemented coda-normalization method, proposed by Aki [1980] and extended by Yoshimoto et al., [1993]. Considering coda-waves to be constituted by back scattered S-waves from heterogeneities, the amplitude of S-waves is normalized by coda amplitude, measured at identical frequency bands.

Choosing the lapse time (t_c) to be more than twice of S-wave travel time (t_s) which is measured from source origin time, the coda-spectral amplitude is found to vary proportionately with source spectral amplitude (e.g., $A_S(f)$ or $A_P(f)$)

$$A_C(f, t_c) \propto A_S(f) \propto A_P(f) \quad (1).$$

Equation 1 is the same as Equation 7 [Yoshimoto, 1993]. The expression indicates that we can apply the spectra of coda wave to normalize the spectra of body waves. This is the premise for the extension of Aki [1980] formulations for S-waves. This method assumes that the scattering coefficient in the area is constant. As seen in Figure 1, the events are distributed in random direction nearby the receiver sites that is under consideration. Negi et al., [2014] opined that such kind of spreading supports in the elimination of the impact of source radiation effect to the optimal degree. Furthermore, the adoption of this method nullifies the instrument response, source effects and site amplification terms since they are inherent to both direct and coda-waves [Molnar et al., 1973; Rautian et al., 1978, Kumar et al., 2014, Bora and Biswas, 2017].

If $A_P(f, r)$ and $A_S(f, r)$ represents the maximum amplitudes of direct P- and S-wave, respectively, and $A_C(f, t_c)$ be the rms value of coda spectral amplitude, then from taking the average of above-mentioned coda normalization method, Q_P and Q_S can be obtained by using the following equations:

$$\left\langle \ln \left[\frac{A_P(f, r)r}{A_C(f, t_c)} \right] \right\rangle = \frac{-\pi f}{Q_P(f)V_P} r + \text{const}(f) \quad (2)$$

$$\left\langle \ln \left[\frac{A_S(f, r)r}{A_C(f, t_c)} \right] \right\rangle = \frac{-\pi f}{Q_S(f)V_S} r + \text{const}(f) \quad (3)$$

where f is frequency, r is the average hypocentral distance, V_P is the average P-wave velocity, and V_S is the average S-wave velocity. As reported by Aki [1980], if we use several P and S waves of the recorded events

having diverse azimuth values, then we can neglect the influence of source radiation pattern which is one vital assumption in the inference of the above 2 equations. Yoshimoto et al., [1993] suggested that the geometrical spreading $Z(r)$ acts as a significant factor as it influences the amplitude decline rate of seismic wave. $Z(r)$ is proportional to $r^{-\alpha}$ (where α is the geometrical spreading factor). In our study region, we assumed α to be unity.

It is obvious from the above equations (2 and 3) that the values of A_S , A_P are functions of frequency and hypocentral distance (r). As soon as we computed A_S , A_P and A_C from the recorded earthquake data, the values of Q_P and Q_S can also be resolved at different central frequencies from the slopes of regression analysis, corresponding to the Equation 2 and Equation 3. It has been observed that Q increases with frequency (>1 Hz). This behavior can be described by a power law

$$Q = Q_0 f^n \quad (4)$$

where Q_0 is value of Q at 1 Hz, f is frequency and n is the frequency-dependent coefficient.

Taking logarithm of Equation 4 it becomes,

$$\log(Q(f)) = n \log(f) + \log(Q_0) \quad (5)$$

Once the value of $Q(f)$ is known for a wide range of frequencies (f), the values of Q_0 and n can be determined for P and S waves in a medium.

5. DATA ANALYSIS

We used vertical-component seismograms for the P-wave and the north-south component for the S-wave investigation, since the maximum amplitudes of S wave are nearly equal in both north-south and east-west components. Based on the seismograms, we calculated the direct P and S wave's amplitudes in a 1.28-s time window.

Five different Butterworth band pass filters were applied to the seismograms (Table 2) that filter the separated ground motion. This is followed by determining the peak to peak amplitude and half of that value is assigned to be $A_P(f, r)$ and $A_S(f, r)$ for P and S waves respectively. Coda-spectral amplitude $A_C(f, t_c)$ is calculated from north-south component within a 1.28-s time window. We choose the peak values, so that we can have the highest fluctuation of the body wave. The time window

Low Value (Hz)	Central Frequency (Hz)	High Value (Hz)
1	1.5	2
2	3.5	5
4	6	8
6	9	12
9	12	15

TABLE 2. Values of band-pass filter used in this study.

for Coda-spectral amplitude was calculated from the twice of the onset of S wave arrival. Following Gupta et al., [1984], the P and S wave velocities are affixed at 6 km/s and 3.5 km/s, respectively.

6. RESULTS AND DISCUSSION

As stated earlier, the extended version of coda normalization method [Yoshimoto et al., 1993], is deployed to estimate Q_p and Q_s . Least-squares fitting and the slopes estimations are applied to keep the deviation to minimum. Accordingly, we calculated Q_p and Q_s using the following relations

$$\text{Slope} = \frac{-\pi f}{Q_p(f)V_p} \text{ for } P\text{-wave} \quad \text{from Equations (2)} \quad (6)$$

$$\text{Slope} = \frac{-\pi f}{Q_s(f)V_s} \text{ for } S\text{-wave} \quad \text{from Equations (3)} \quad (7)$$

The optimal fitting lines are plotted in Figure 3 for TZR station. We observe that Q_p and Q_s exhibit an increase proportionately with in frequency, implying exclusive dependence on frequency (Table 3). At frequency of 1.5 Hz, Q_p and Q_s are found to be 76 and 171. While the estimates plunge to 1097 and 2936 for Q_p and Q_s , respectively at 12 Hz. Figure 4 (a and b) illustrate the variation of Q_p and Q_s at all the receiver stations. There is no correlation with tectonic or geological features for Q_p and Q_s for frequency 1.5 Hz as indicated by Figure 4. Identical results arise for other frequencies. Apart from this, no reasonable differences appear in Q_p and Q_s at a given frequency among the stations. As such, the average values of Q_p and Q_s

are computed by taking mean over respective values at all station shown in Figure 5, with standard deviation enlisted in Table 3. It can be observed that smaller standard deviations arise for low frequencies than high frequencies. The standard deviations in Q , as shown in Figure 5 and listed in Table 3, increase when the frequency increases. The standard deviations are physically caused by focusing or defocusing of seismic waves as a result of heterogeneities in the lithosphere. As per Frankel and Wennerberg [1987], the scatters in the amplitudes of direct waves are ascribed to other processes rather than scattering and intrinsic attenuation; in spite of smoothing the radiation pattern by considering a huge sets of earthquake events. In the media, where velocity increases with depth, the geometrical spreading is inversely proportional to the hypocentral distance. This produces substantial loss in the amplitude of direct waves. Besides, the variation in azimuth of earthquake locations is also a possible reason for the scatter effect.

The value of $Q_s/Q_p > 1$ for the frequency range 1.5-12 Hz is assessed for this study. Similar results were also reported by Rautian et al., [1978] and Yoshimoto et al., [1993]. They obtained same results at higher frequency levels. Equivalent estimates are also found for South Eastern Korea [Chung and Sato, 2001] for a frequency range of 1.5 to 10 Hz, where the ratio is established to be greater than 1. The obtained value of Q_s/Q_p in our study regions agrees with the outcomes reported by the other studies as mentioned above. We found that $Q_s > Q_p$ by a factor of 2.44 in 1.5-12 Hz range, which agrees well with the theoretically expected ratio of 2.41 for whole north-eastern part of India [Sato, 1984].

With a power law of the form $Q = Q_0 f^n$, where n is the frequency-dependence coefficient and Q_0 is the quality factor at $f=1\text{Hz}$, we estimated Q_0 and n (Table 4). The value of n is approximately close to 1 and varies because of heterogeneity of the medium from area to area Aki [1981]. The power law fitting yields $Q_p = (45 \pm 3)f^{(1.3 \pm 0.07)}$ and $Q_s = (101 \pm 4)f^{(1.4 \pm 0.05)}$ for the study region. The low estimates can be correlated with the seismically active nature of this fault [Bora et al., 2017b].

We observed that within the entire frequency range, the estimated values of Q_s is more than Q_p . This implies that for this study area, P waves are attenuated more than that of S waves. As reported by Bianco et al., [1999] and Sato and Fehler [1998], the attained

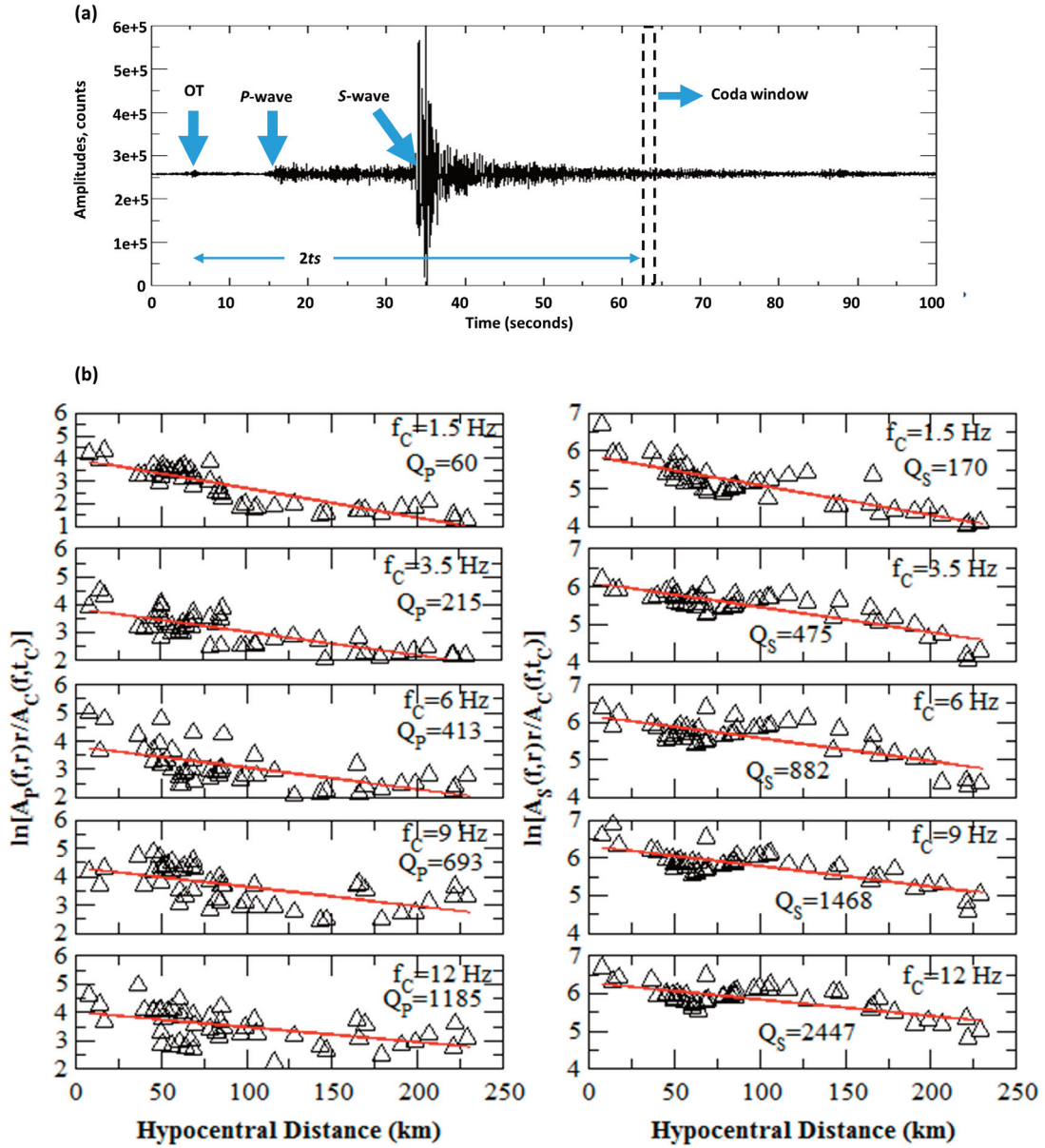


FIGURE 3. (a) The plot of typical seismogram. Arrows indicates origin time, P-wave and S-wave arrival, while coda waves are indicated by dashed line. (b) Coda normalized P and S wave amplitude entailing vertical and north-south component of seismogram within each frequency band for TZR station. The estimated Q_p and Q_s values are also shown.

$Q_s/Q_p > 1$ is also observed in the upper crust of various other areas, having a higher amount of lateral heterogeneity. This has direct relation with disparities pertinent to this region. Blending geological aspect, varied level of disparities can also be taken into account.

Van Eck [1988] proposed an interrelation among the level of tectonic activity and the degree of frequency dependence. It has been noticed from the reported literature [Roecker et al., 1982; Rodriguez et al.,

1983; Havskov et al., 1989] that seismically active provinces are generally characterized by low Q_0 values and high n values; while stable regions are described by high Q_0 and low n values [Pujades et al., 1991; Pulli, 1984 and Rhea, 1984].

In order to validate the results, we attempted correlation of them with the available geophysical confirmations, reported by other researchers for this entire region. It can be gleaned from reports of Bhattacharya et al., [2002, 2008] that KF could be cited

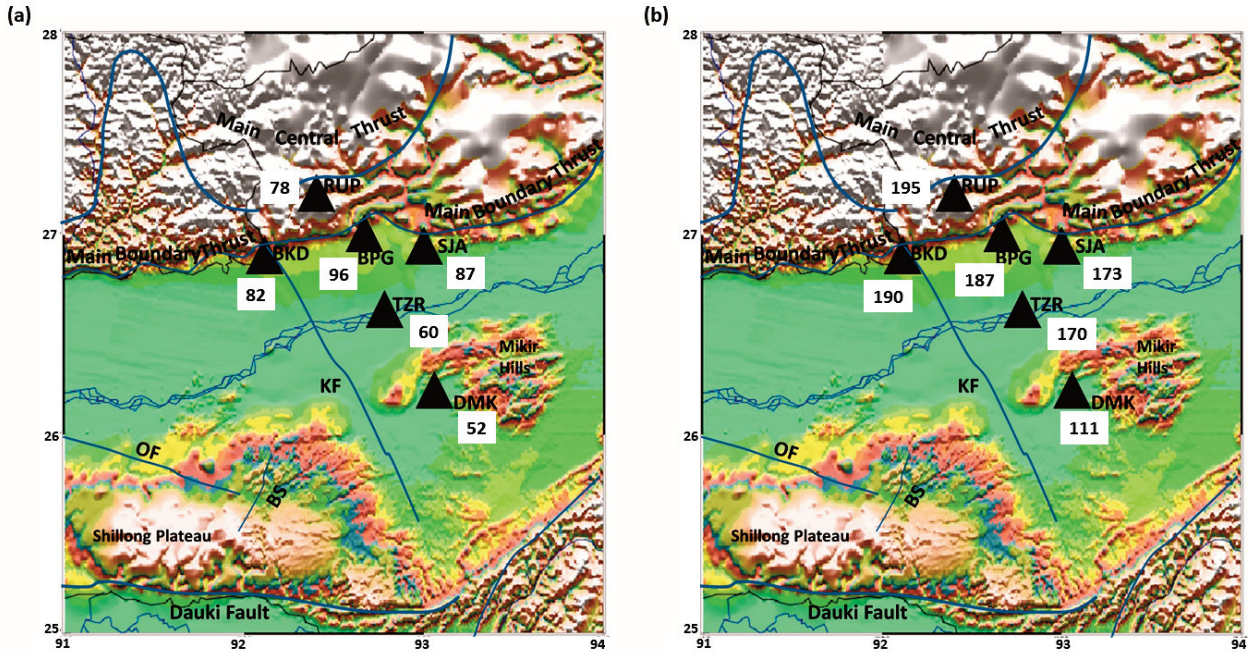


FIGURE 4. Estimates of (a) Q_p and (b) Q_s at central frequency 1.5 Hz mentioned besides each stations.

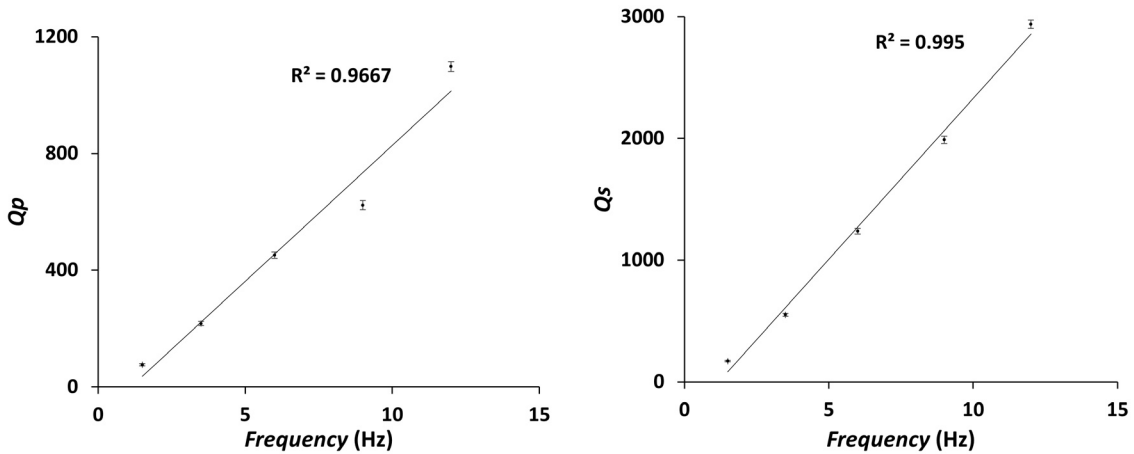


FIGURE 5. Variation of Q_p and Q_s versus f for Kopili zone with error bars.

as the next prominent active zone after Shillong Plateau in the NE-India. They detected a considerable seismic activity along the northwestern-south eastern margin of KF. Additionally, Bhattacharya et al., [2002] had done 1D and 2D mapping of whole NE region. They found high b-value and high fractal dimensions ($1.65 < D < 1.85$) beside the KF. It is already established by Mogi [1962] that high b-value signifies complex heterogeneities or the existence of rock mass with variegated fractures. The higher D-values beside the KF can also be ascribed to the heterogeneous transverse structure of this fault [Bhattacharya et al., 2002, 2008].

7. COMPARISON WITH GLOBAL DATA

To build an in-depth understanding, we carried out an investigation to discern a global perspective in the context of quality factors related to P and S waves. To this end, we made a plot in Figure 6(a) and (b), respectively comparing our findings with those estimated for other parts of the globe having diverse tectonic settings. Based on attenuation features, the categorization was executed. The pattern of Q_p with respect to frequency is identical (Figure 6(a)) to the estimates found in other tectonic regions, showing a rise in Q_p values with increasing frequency. The increase

f (Hz)	Q_p	$\pm\Delta Q_p$	Q_s	$\pm\Delta Q_s$	Q_s/Q_p
1.5	76	4.0	171	5.6	2.2
3.5	216	7.6	551	10.7	2.5
6	451	10.7	1239	23.4	2.7
9	623	15.1	1988	30.0	3.1
12	1098	17.1	2937	33.0	2.6

TABLE 3. Average estimates of Q_p and Q_s along with their SD.

Serial no	Station	Q_0 (for P)	$\pm \Delta Q_0$	n	$\pm n$	Q_0 (for S)	$\pm \Delta Q_0$	n	$\pm n$
1	BKD	59	3	1.05	0.07	122	3.2	1.19	0.03
2	BPG	52	4	1.16	0.1	115	2.4	1.2	0.03
3	DMK	28	2	1.39	0.09	63	1.8	1.49	0.03
4	RUPA	45	2	1.5	0.06	112	3.3	1.3	0.04
5	SJA	48	2	1.3	0.06	95	7	1.7	0.09
6	TZR	35	1.19	1.4	0.04	100	3.5	1.3	0.04

TABLE 4. Values of Q_0 for P and S along with their n values at all the six stations.

in Q values with increasing frequency indicates the frequency-dependent nature of the Q estimates in the region. It suggests that the attenuation characteristics in the KF zone are well comparable to the other seismically active

values is ascribed to distinct regional behavior of the attenuation mechanism [Lees and Lindley, 1994]. It is evident that our result falls into the region of $Q_s > Q_p$. Lees and Lindley [1994] theoretically showed that Q_p equals 2.25

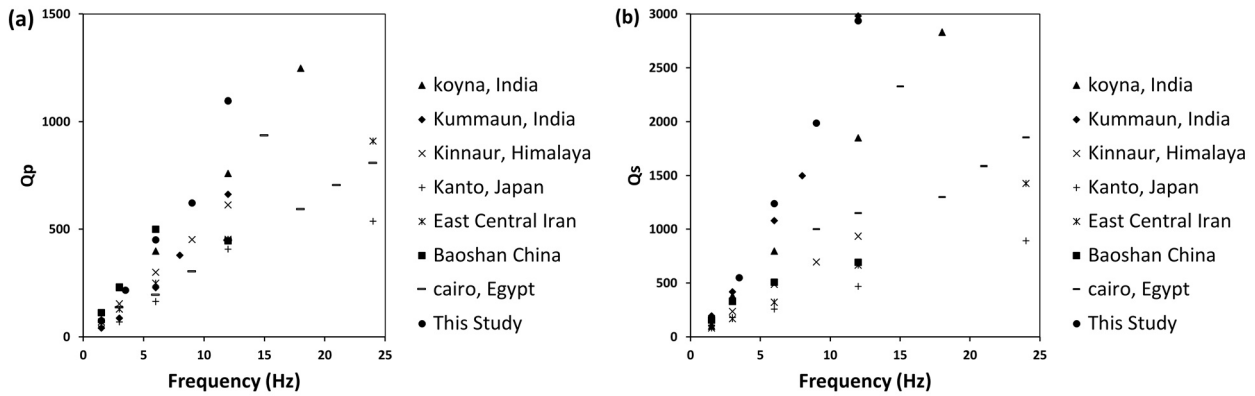


FIGURE 6. Global comparison of estimates of (a) Q_p and (b) Q_s with different tectonic settings.

regions of the world. However, the lower estimates of Q_p are primarily accredited to complex degree of crustal heterogeneities. Similarly, in Figure 6(b), it is seen that the pattern of Q_s exhibits an identical pattern as found in Kummaun, India.

Figure 7 gives an illustrative valuation of average estimates Q_s/Q_p ratio of our study area to previous studies of various locations at 1 Hz. The disperse nature of Q_s/Q_p

times of Q_s (i.e. $Q_s/Q_p = 4/9$) for entire world crust. Keeping this equivalence of Q_p with Q_s , a benchmark has been plotted in Figure 7, represented by dashed line. The solid line indicates $Q_s = Q_p$. However, the ratios so far, reported worldwide considerably diverge from this theoretical value. Yoshimoto et al., [1993] revealed that $Q_s/Q_p > 1$ for low frequency (0.1 Hz) seismic waves. For the frequencies in the range of 1Hz to 30 Hz, Yoshimoto et al., [1998]

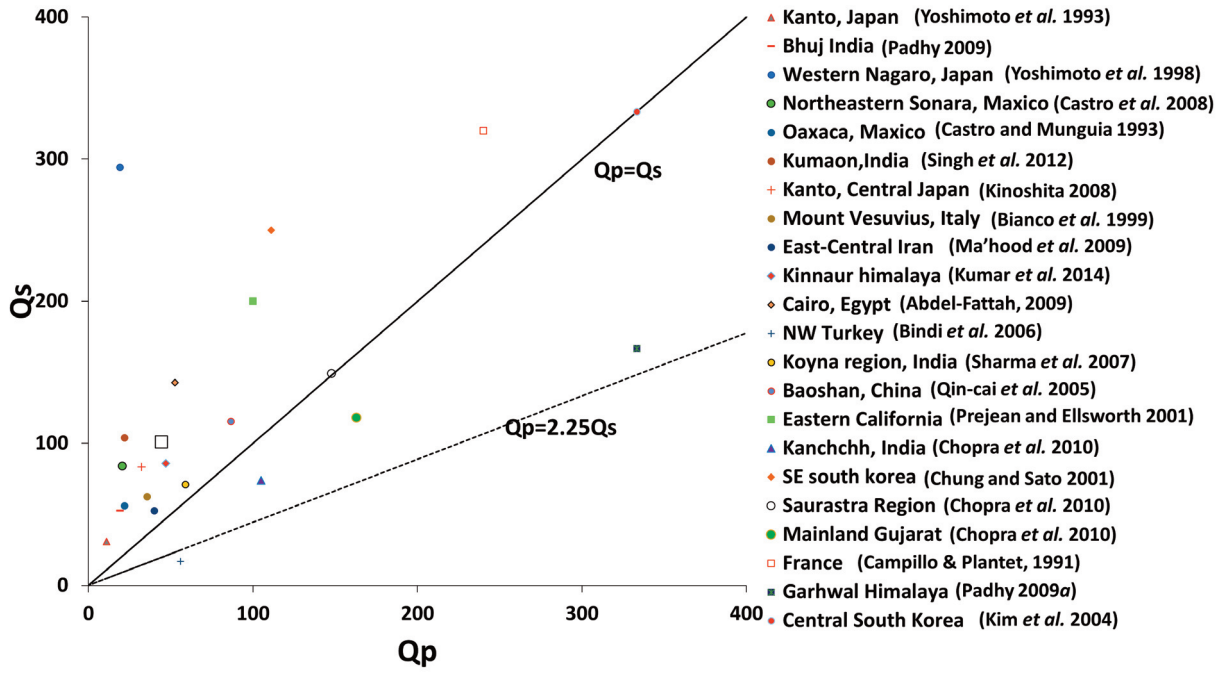


FIGURE 7. Global plot of Q_p versus Q_s along with the current study (at 1 Hz). The small square representing the estimated value in our study.

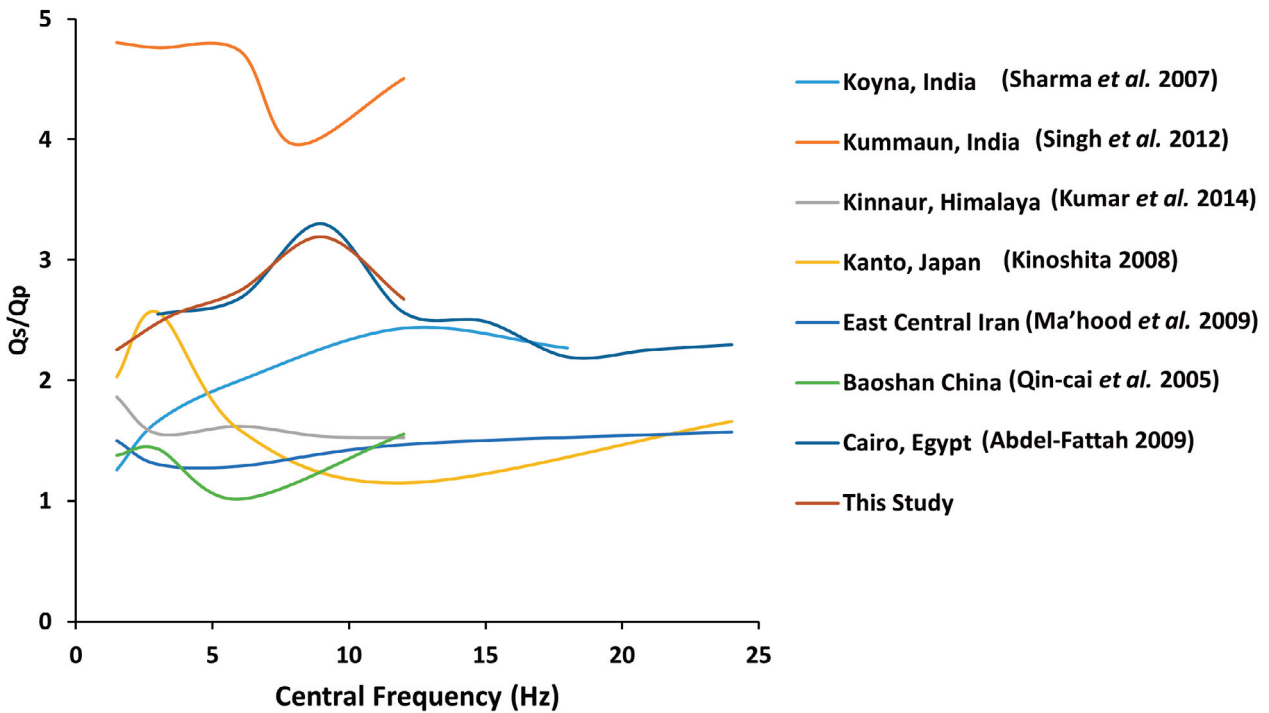


FIGURE 8. Comparison of estimated Q_s/Q_p ratio as a function of frequencies with those of different tectonic parts of the world.

opined that $Q_s/Q_p > 1$.

This has been also obtained worldwide [Castro and Munguia, 1993; Chung and Sato, 2001; Kinoshita, 2008; Padhy, 2009; Abdel-Fattah, 2009]. Recently, Kumar *et al.*, [2014] reported $Q_s/Q_p > 1$ for the Kinnaur Himalaya region for frequencies ranging from 1.5 to 12 Hz. Therefore, the

derived Q_s/Q_p ratio tallies well with other values reported worldwide. We have also plotted a comparison of Q_s/Q_p which was computed at diverse frequencies with those conducted at other tectonic regions worldwide in Figure 8. In the frequency range of 1.5 to 12 Hz, our estimate corroborates well with dissimilar regions of the sphere.

8. CONCLUSIONS

In conclusion, we have carefully delineated the attenuation features of Kopili Region, emphasizing frequency dependent behavior.

The results establish higher values of Q for S waves ($Q_S = (101 \pm 4)f^{(1.4 \pm 0.05)}$) than for P waves ($Q_P = (45 \pm 3)f^{(1.3 \pm 0.07)}$) in the 1.5-12 Hz frequency band. It is seen that our findings agree with other published results on tectonically active regions that is characterized by high degree of heterogeneity. Hence, it can be useful for further studies in ground motion prediction in Kopili region. The low value of quality factors corresponding to P and S waves refers to seismically active areas with complex heterogeneity. The estimated value of Q_S/Q_P and their subsequent association with frequency affirm the dominance of scattering as a major contribution to diminution of seismic amplitudes. This study will act as a basic building to grasp attenuation mechanism, prevailing here. It will also help to restrain the frequency dependence of body wave attenuation in the earth's crust, which is important to modify the velocity dispersion due to attenuation. Furthermore, attenuation study of a region is considered as an integral part for seismic hazard assessment, source parameter studies and ground motion simulation process. There are many quality factors reported for whole northeast India, which is a unique combination of different tectonic units. So assigning a single Q for entire northeast India is not justified. The current work indeed finds a quality factor for Kopili fault zone, so the new quality factors will prove beneficial for above mentioned seismological practices.

Acknowledgements. The Editor Prof. Federica Riguzzi and the anonymous reviewers, whose comments helped in improving the quality of the current manuscript significantly, are sincerely acknowledged. Author NB is thankful to the Ministry of Earth Science (MoES) for providing financial support [through grant number MoES/P.O.(Seismo)/1(214)/2014].

REFERENCES

Abdel-Fattah AK (2009) Attenuation of body waves in the crust beneath the vicinity of Cairo Metropolitan area (Egypt) using coda normalization method. *Geophysical Journal International*. 176:126-134.

- Aki K (1969) Analysis of seismic coda of local earthquakes as scattered waves. *Journal of Geophysical Research*. 74:615-631.
- Aki K, Chouet B (1975) Origin of coda waves: source, attenuation and scattering effects. *Journal of Geophysical Research*. 80:3322-3342.
- Aki K (1980) Attenuation of shear-waves in the lithosphere for frequencies from 0.05 to 25 Hz. *Physics of the Earth and Planetary Interiors* 21:50-60.
- Aki, K.,(1981) Attenuation and scattering of short-period seismic waves in the lithosphere, Identification of seismic sources-Earthquake or Underground Explosion, eds.: Husebye, E.S., and Mykkeltveit, S., D. Reidel Publishing Co., pp. 515-541.
- Bhattacharya, P.M., Majumder, R.K. and Kayal, J.R., 2002. Fractal dimension and b-value mapping in northeast India, *Current Science*. 82, 1486-1491.
- Bhattacharya PM, Pujol J, Mazumdar RK, Kayal JR (2005) Relocation of earthquakes in the Northeast India region using joint Hypocenter determination method. *Curr Sci* 89(8):1404- 1413
- Bhattacharya, P.M., Mukhopadhyay, S., Majumdar, R.K. and Kayal, J.R., 2008. 3-D seismic structure of the northeast India region and its implications for local and regional tectonics, *Journal of Asian Earth Sciences*. 33, 25-41.
- Bianco F, Castellano M, Del Pezzo E, Ibañez JM (1999) Attenuation of short-period seismic waves at Mt. Vesuvius, Italy. *Geophysical Journal International*. 138:67-76
- Biswas, R. Baruah, S. Bora, D. Kalita, A And Baruah, S. (2013 a), The Effects of Attenuation and Site on the Spectra of Microearthquakes in the Shillong Region of Northeast India, *Pure and Applied Geophysics*, Springer Basel. 170: 1833.
- Biswas, R. Baruah, S. Bora, D. (2013 b), Influence of Attenuation and Site on Microearthquakes' Spectra in Shillong Region, of Northeast, India: A Case Study, *Acta Geophysica*, vol. 61, no. 4, Aug. 2013, pp. 886-904, DOI: 10.2478/s11600-013-0129-x
- Biswas, R., Bora, N., Baruah, S., 2018a. Frequency dependent site response inferred from microtremors accompanied by ambient noise. *Phys Astron Int J* 2(4):273-277. <https://doi.org/10.15406/paij.2018.02.00098>.
- Biswas, R., Baruah, S. and Bora, N., 2018b. Assessing shear wave velocity profiles using multiple passive techniques of Shillong region of northeast India. *Nat Hazards*. 94(3):1023-1041.

- <https://doi.org/10.1007/s11069-018-3453-2>.
- Bora, N., and Biswas, R. 2017. "Quantifying Regional Body Wave Attenuation in a Seismic Prone Zone of Northeast India." *Pure and Applied Geophysics*, 174(5): 1953-63.
- Bora, N., Biswas, R., and Bora, D. 2017 a, "Assessing attenuation characteristics prevailing in a seismic prone area of NE India". *J. Geophys. Eng.* 14:1368-1381, DOI: <https://doi.org/10.1088/1742-2140/aa7d11>
- Bora, N., Biswas, R., and Dobrynina A. A., 2017 b, "Regional variation of coda Q in Kopili fault zone of northeast India and its implications". *Tectonophysics*. 722 (2018) 235-248, DOI: <https://doi.org/10.1016/j.tecto.2017.11.008>
- Bora, N., and Biswas, R., 2019. Delineation of subsurface profiles beneath the Kopili fault zone in northeast India utilizing coda portion, *Journal of Asian Earth Sciences*, <https://doi.org/10.1016/j.jseaes.2019.01.023>.
- Campillo, M. and Plantet, J.L., 1991. Frequency dependence and spatial distribution of seismic attenuation in France: experimental results and possible interpretations, *Physics of the Earth and Planetary Interiors*, 67, 48-64.
- Castro RR, Munguia L (1993) Attenuation of P and S waves in the Oaxaca, Mexico, subduction zone. *Physics of the Earth and Planetary Interiors*. 76:179-187
- Chopra S, Kumar D, Rastogi BK (2010) Attenuation of high frequency P and S waves in the Gujarat Region, India. *Pure and Applied Geophysics*. 168:797-813
- Chung TW, Sato H (2001) Attenuation of high-frequency P and S waves in the crust of southeastern South Korea. *Bulletin of the Seismological Society of America*. 91:1867-1874.
- Frankel, A. and Wennerberg, L., 1987. Energy-flux model of seismic coda: Separation of scattering and intrinsic attenuation, *Bull. Seismol. Soc. Am.*, 77, 1223-1251.
- Gupta, H.K., Singh, S.C., Dutta, T.K. and Saikia, M.M., 1984. Recent investigations of North East India seismicity, in *Proceedings of the International Symposium on Continental Seismicity and Earthquake Prediction*, pp. 63-71, eds Gongu, G., Xing-Yuan, M., Seismological Press, Beijing.
- Havskov J, Malone S, McClurg D, Crosson R (1989) Coda Q for the State of Washington. *Bulletin of the Seismological Society of America*. 79:1024-1038.
- Hermann R (1980) Q estimates using coda of local earthquakes. *Bulletin of the Seismological Society of America*. 70:447-468.
- Hoshiaba, M., H. Sato and M. Fehler (1991). Numerical basis of the separation of scattering and intrinsic absorption from full seismogram envelope - a Monte-Carlo simulation of multiple isotropic scattering, *Pap. Meteorol. Geophys.*, 42, 65-91.
- Hough SE, Anderson JG (1988) High-frequency spectra observed at Anza, California: implications for Q structure. *Bulletin of the Seismological Society of America*. 78:692-707
- Kim KD, Chung TW, Kyung JB (2004) Attenuation of high frequency P and S waves in the crust of Choongchung provinces, Central South Korea. *Bulletin of the Seismological Society of America*. 94:1070-1078
- Kinoshita S (2008) Deep-borehole-measured Q_p and Q_s attenuation for two Kanto sediment layer sites. *Bulletin of the Seismological Society of America*. 98:463-468
- Knopoff, L., and J. A. Hudson, (1964). Scattering of elastic waves by small inhomogeneities, *J. Acoust. Soc. Am.*, 36, 471-476, 1964.
- Kayal, J.R., Arefiev, S.S., Barua, S., Hazarika, D., Gogoi, N., Kumar, A., Chowdhury, S.N., Kalita, S., (2006). Shillong Plateau earthquakes in Northeast India region: complex tectonic model. *Current Science*. 91 (1), 109-114.
- Kayal, J.R., Arefiev, S.S., Baruah, S., Tatevossian, R., Gogoi, N., Sanoujam, M., Gautam, J.L., Hazarika, D., And Borah, D. (2010), The 2009 Bhutan and Assam felt earthquakes (Mw 6.3 and 5.1) at the Kopili fault in the northeast Himalaya region, *Geomatics, Natural Hazards and Risk*. 1(3), 273- 281
- Kumar Devender, Reddy D.V., Pandey Anand K. (2016), Paleoseismic investigations in the Kopili Fault Zone of North East India: Evidences from liquefaction chronology, *Tectonophysics*. 674, 65-75.
- Kumar Naresh, Mate S., Mukhopadhyay S. (2014), Estimation of Q_p and Q_s of Kinnaur Himalaya. *Journal of Seismology*. 18:47-59.
- Kundu B, Gahalaut VK. (2013). Tectonic geodesy revealing geodynamic complexity of the Indo-Burmese arc region, north east India. *Curr Sci*. 104:920-933.
- Lees JM, Lindley GT (1994) Three-dimensional attenuation tomography at Loma Prieta: inversion of t^*

- for Q . *Journal of Geophysical Research*. 99:6843-6863
- Ma'hood M, Hamzehloo H, Doloei GJ (2009) Attenuation of high frequency P and S waves in the crust of the East-Central Iran. *Geophysical Journal International*.179:1669-1678
- Masuda, T., 1988. Corner frequencies and Q values of P waves by simultaneous inversion technique, *Science reports of the Tohoku University, 5th Series Geophysics*, 31, 101-125.
- Mitchell BJ (1995) Anelastic structure and evolution of the continental crust and upper mantle from seismic surface wave attenuation. *Reviews of Geophysics*. 33:441-462
- Mogi, K., 1962. Magnitude-frequency relationship for elastic shocks accompanying fractures of various materials and some related problems in earthquakes. *Bulletin of the Earthquake Research Institute. University of Tokyo*, 40: 831-883.
- Molnar P, Tucker BE, Brune JN (1973) Corner frequencies of P and S waves and models of earthquake sources. *Bulletin of the Seismological Society of America*. 63:2091-2104
- Mukhopadhyay S, Sharma J (2010) Attenuation characteristics of Garwhal-Kumaun Himalayas from analysis of coda of local earthquakes. *Journal of Seismology*. 14:693-713. doi:10.1007/s10950-010-9192-9
- Negi, S. S., Paul, A., Joshi, A. and Kamal, 2014. *Body wave crustal attenuation in the Garhwal Himalaya, India Pure Appl. Geophysics*, Springer Basel.
- Oldham, R.D. (1899), Report on the great earthquake of 12th June 1897. *Mem Geological Survey of India*. 29, 1-379.
- Padhy S (2009) Characteristics of body wave attenuations in the Bhuj crust. *Bulletin of the Seismological Society of America*. 99:3300-3313
- Padhy, S., 2009a. Inversion of seismogram envelopes using a multiple isotropic scattering model in Garhwal Himalaya, *Bulletin of the Seismological Society of America*., 99, 726-740.
- Padhy, S. and Subhadra, N., 2010. Attenuation of high-frequency seismic waves in northeast India, *Geophysical Journal International*., 181, 453-467.
- Poddar, M.C., 1950. The Assam earthquake of 15th August 1950. *Indian Miner*. 4,167-176.
- Prejean SG, Ellsworth WL (2001) Observations of earthquake source parameters and attenuation at 2 km depth in the Long Valley Caldera, eastern California. *Bulletin of the Seismological Society of America*. 91:165-177
- Pujades, L., Canas, J. A., Egozcue, J. J., Puigvi, M. A., Pous, J., Gallart, J., Lana, X. and CASAS, A, (1991), Coda Q distribution in Iberian Peninsula, *Geophysical Journal International*.100, 285-301.
- Pulli JJ (1984) Attenuation of coda waves in New England. *Bulletin of the Seismological Society of America*. 74:1149-1166
- Qin-cai, W., Jie, L., Si-hua, Z. and Zhang-li, C., 2005. Frequency-dependent attenuation of P and S waves in Yunnan region, *Acta Seismologica Sinica*. 18, 632-642.
- Rautian TG, Khalturin VI (1978) The use of coda for determination of the earthquake source spectrum. *Bulletin of the Seismological Society of America*. 68:923-948
- Rautian TG, Khalturin VI, Martynov VG, Molnar P (1978) Preliminary analysis of the spectral content of P and S waves from local earthquakes in the Garm, Tadjikistan region. *Bulletin of the Seismological Society of America*. 68:949-971
- Rhea, S. (1984), Q determined from local earthquakes in South Carolina coastal plain, *Bulletin of the Seismological Society of America*. 74, 2257-2268.
- Rodriguez, M., Havskov, J. and Singh, S. K. (1983), Q from coda waves near Petatlan, Guerrero, Mexico, *Bulletin of the Seismological Society of America*. 74, 2257-2268.
- Roecker, S. W., Tucker, B., King, J. and Hartzfeld, D. (1982), Estimates of Q in Central Asia as a function of frequency and depth using the coda of locally recorded earthquakes, *Bulletin of the Seismological Society of America*. 72, 129-149.
- Sato H, Fehler M (1998). *Seismic wave propagation and scattering in the heterogeneous earth*. (AIP) American Institute of Physics. Press/Springer, New York, p 308
- Sato H. (1992). Thermal structure of the mantle wedge beneath Northeastern Japan: Magmatism in an island arc from the combined data of seismic anelasticity and velocity and heat flow. *Journal of Volcanology and Geothermal Research*. 51: 237~252.
- Sato, H. and Matsumura, S., 1980. $Q-1$ value of S-waves under the Kanto district in Japan, *Zisin (Journal of the Seismological Society of Japan*. 2nd ser), 33, 541-543.
- Sato, H., 1984. Attenuation and envelope formation of three-component seismograms of small local

- earthquakes in randomly inhomogeneous lithosphere, *Journal of Geophysical Research*. 89, 1221-1241.
- Scherbaum, F. and Sato, H., 1991. Inversions of full seismologic envelopes based on the parabolic approximations: estimation of randomness and attenuation in the southeast Honshu, Japan. *Journal of Geophysical Research*. 96, 2223-2232.
- Sharma B, Teotia SS, Kumar D (2007) Attenuation of P, S, and coda waves in Koyna region, India. *Journal of Seismology*. 11:327-334
- Singh C, Singh A, Bharathi VKS, Bansal AR, Chadha RK (2012) Frequency-dependent body wave attenuation characteristics in the Kumaun Himalaya. *Tectonophysics*. 524:37-42
- Takemura M, Kato K, Ikeura T, Shima E (1991) Site amplification of S waves from strong motion records in special relation surface geology. *Journal of Physics of the Earth*. 39:552-573
- Tsujiura M (1966) Frequency analysis of the seismic waves. *Bulletin of the Earthquake Research Institute, Tokyo University*, 44:873-891
- Van Eck, T. (1988), Attenuation of coda waves in Dead Sea region, *Bulletin of the Seismological Society of America*. 78, 770-779.
- Yoshimoto K, Sato H, Ohtake M (1993) Frequency-dependent attenuation of P and S waves in the Kanto Area, Japan, based on the coda-normalization method. *Geophysical Journal International*. 114:165-174
- Yoshimoto K, Sato H, Ito Y, Ito H, Ohminato T, Ohtake M (1998) Frequency-dependent attenuation of high-frequency P and S waves in the upper crust in western Nagano, Japan. *Pure and Applied Geophysics*. 153:489-502
- Wu, R.S. (1985). Multiple scattering and energy transfer of seismic waves: separation of scattering effect from intrinsic attenuation, I, theoretical model, *Geophysical Journal of the Royal Astronomical Society*, 82, 57-80.

*CORRESPONDING AUTHOR: Rajib BISWAS,
Geophysical Lab, Department of Physics, Tezpur University
Tezpur, Assam, India

email: rajib@tezu.ernet.in

© 2019 the Istituto Nazionale di Geofisica e Vulcanologia.
All rights reserved